

Dynamic properties of microemulsions modified with homopolymers and diblock copolymers: The determination of bending moduli and renormalization effects

Olaf Holderer, Henrich Frielinghaus, Dmytro Byelov, Michael Monkenbusch, Jürgen Allgaier, and Dieter Richter

Institut für Festkörperforschung, Forschungszentrum Jülich GmbH, D-52425 Jülich, Germany

(Received 11 November 2004; accepted 15 December 2004; published online 28 February 2005)

The properties of bicontinuous microemulsions, consisting of water, oil, and a surfactant, can be modified by the addition of diblock copolymers (boosting effect) and homopolymers (inverse boosting effect) or a combination of both. Here, the influence of the addition of homopolymers (PEP_X and PEO_X, $X=5k$ or $10k$ molecular weight) on the dynamics of the surfactant layer is studied with neutron spin echo spectroscopy (NSE). Combining the results with the previous findings for diblock copolymers allows for a better separation of viscosity and bending modulus effects. With the addition of homopolymers, a significant increase of the relaxation rate compared to the pure microemulsion has been observed. The influence on the bending rigidity κ is measured with NSE experiments. Homopolymer addition reduces κ by up to $\Delta\kappa \approx -0.5k_B T$, whereas the diblock copolymer yields an increase of κ by $\sim 0.3k_B T$. Comparison of the bending moduli that are obtained by analysis of the dynamics to those obtained from small angle neutron scattering (SANS) sheds light on the different renormalization length scales for NSE and SANS. Variation of the surfactant concentration at otherwise constant conditions of homopolymer or diblock-copolymer concentration shows that NSE results are leading to the pure bending rigidity, while the renormalized one is measured with SANS. © 2005 American Institute of Physics. [DOI: 10.1063/1.1857523]

I. INTRODUCTION

Mixtures of water, oil, and a surfactant can form thermodynamically stable microemulsion phases. The water and oil phases are separated by a monolayer of surfactant molecules. If the same amount of water and oil is present, bicontinuous microemulsions form under certain conditions of temperature and surfactant concentration.¹

Bicontinuous microemulsions can be theoretically described with different approaches, e.g., microscopic lattice models, phenomenological Ginzburg–Landau models or membrane models.² The latter are based on the elastic curvature energy, controlling shape and fluctuations of the interface layer,³

$$F_{\text{el}} = \int dS \left[\frac{\kappa}{2} (c_1 + c_2 - 2c_0)^2 + \bar{\kappa} c_1 c_2 \right]. \quad (1)$$

Here, c_1 and c_2 describe the principal curvatures at each point of the membrane, c_0 is the spontaneous curvature, κ the bending rigidity, and $\bar{\kappa}$ the saddle splay modulus.

The surfactant efficiency of C₁₀E₄ (decyl polyglycol ether) in a bicontinuous microemulsion can be largely enhanced upon addition of a small amount of diblock copolymers (boosting effect) but is decreased when homopolymers are added to the water and oil, respectively. This has been shown experimentally, e.g., in Refs. 4–7 with polyethylenepropylene_X-polyethylenoxide_Y (PEP_X-PEO_Y) as diblock copolymer and in Ref. 8 with the corresponding homopolymers PEP_X and PEO_Y. The boosting effect of the diblock copolymer is explained by a change of the bending

modulus of the surfactant membrane. Inversely, the homopolymers decrease the bending rigidity, as has been shown by small angle neutron scattering (SANS) measurements⁸ and predicted theoretically.⁹ Furthermore they increase the viscosity of oil and water, respectively.

Neutron scattering allows one to investigate the structural and dynamical properties of microemulsions, using the possibility of varying the contrast by the exchange of hydrogen with deuterium. In Fig. 1, such a sample is depicted schematically. In “bulk” contrast (D₂O, *h*-decane, C₁₀E₄), the characteristic average distance between water-water or oil-oil domains d , and furthermore the correlation length ξ of the microemulsion, can be determined by SANS from fits of the scattering curve with the formula proposed by Teubner and Strey,^{10,11}

$$S(q) \propto \frac{1}{q^4 - 2(q_0^2 - \xi^{-2})q^2 + (q_0^2 + \xi^{-2})^2}. \quad (2)$$

Here, q is the momentum transfer in the scattering process, and $q_0 = 2\pi/d$ determines the characteristic length d . The scattering function, Eq. (2), follows from a Ginzburg–Landau approach¹⁰ and has a correlation peak close to q_0 . The width of the peak is determined by ξ . By matching the free energy expression derived from a Gaussian random field model to the Ginzburg–Landau approach which leads to the Teubner–Strey formula, a relation between the renormalized bending rigidity $\kappa_R = \kappa_{\text{SANS}}$ and the structural parameters d and ξ can be derived,^{6,12}

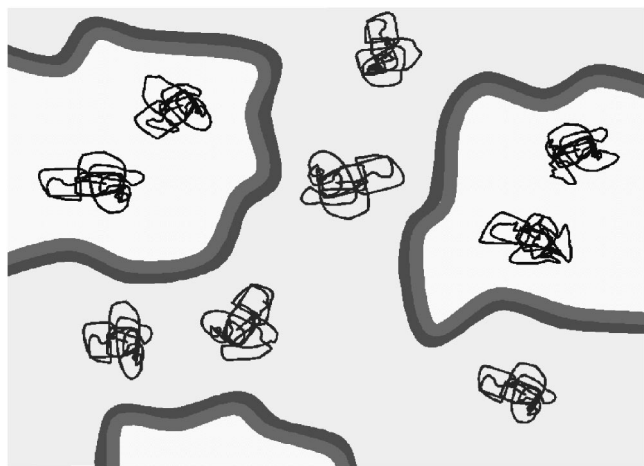


FIG. 1. Schematic drawing of a bicontinuous microemulsion, consisting of equal amounts of oil and water, separated by the amphiphilic surfactant $C_{10}E_4$. The homopolymers PEO and PEP have been added to the water and oil phase, respectively.

$$\frac{2\pi}{d}\xi = \frac{64}{5\sqrt{3}} \frac{\kappa_{\text{SANS}}}{k_B T} \Theta(\kappa_{\text{SANS}}, \Psi). \quad (3)$$

Here, we assume $\Theta=1$ which is the limit for large κ (see Ref. 8). The renormalized bending modulus κ_{SANS} lumps all effects from membrane fluctuations up to a wavelength corresponding to the structural dimension into the bending modulus value. It differs from the “bare” bending modulus of the membrane by a renormalization factor, which depends on the structural length scale, here expressed in terms of the volume fraction of the membrane,

$$\kappa_{\text{SANS}} = \kappa_{\text{bare}} + k_B T \frac{\alpha}{4\pi} \ln(\Psi), \quad (4)$$

with the volume fraction Ψ of the surfactant membrane (note¹³: $d \sim \Psi^{-1}$) and a renormalization constant $\alpha=3$ according to Refs. 12 and 14. The bare bending modulus κ_{bare} in this equation includes terms accounting for, e.g., homopolymers in the solution or diblock copolymers decorating the membrane. For a pure microemulsion, κ_{bare} reduces to the bare (nonrenormalized) bending modulus κ_0 of the membrane.

The observation of the dynamics of the surfactant membrane with neutron spin echo (NSE) spectroscopy is best possible in film contrast, i.e., with samples consisting of D_2O , d -decane, and the surfactant $C_{10}E_4$.⁴ The addition of diblock copolymers or homopolymers allows for preparation of series of similar microemulsions with varying κ and structural length, thereby permitting a systematic comparison of results for κ obtained by NSE and SANS. Fits of the data with the corresponding theoretical dynamic structure factor yield the relaxation rate and by further analysis the bending modulus κ_{NSE} of the membrane as described in Sec. III. Since NSE at high q values probes the dynamics of the surfactant membrane on a local scale and the used expression, Eq. (8), includes all contributions from the fluctuation modes explicitly, it must be assumed that κ_{NSE} represents rather the bare bending modulus of the membrane than the renormalized one. The membrane is modified by the addition of

diblock copolymers or homopolymers which results in changes of the bending modulus and eventually also the solvent viscosity. Exploiting the thereby possible parameter variation by combining results on homopolymer microemulsions with the previous findings for block copolymers⁴ yields a better understanding of the relation between polymer addition, bending moduli, and the observed dynamics.

The present work reports a study of the influence of the addition of homopolymers (PEP_X and PEO_X, $X=5k$ or $10k$ molecular weight) on the dynamics of the surfactant layer by NSE, relates these with the effects on the bending moduli and compares the results with previous experiments on samples containing PEP-PEO diblock polymers as cosurfactants.⁴

II. EXPERIMENT

A. Samples

The dynamics of the surfactant layer on a local scale has been investigated in “film contrast,” i.e., with deuterated water, deuterated decane and protonated surfactant, and polymer. Structural parameters from SANS were obtained from the equivalent “bulk contrast” samples (deuterated water, protonated decane) with the same volume fraction of surfactant. All samples contained equal amounts of water and oil with different amounts of surfactant.

For the samples containing homopolymers, water-PEO and decane-PEP solutions have been prepared. Two homopolymer types, polyethyleneoxide (PEO) and polyethylenepropylene (PEP) with two different molecular weights (5 kg/mol and 10 kg/mol) have been dissolved in the water and decane, respectively, in two different volume fractions Φ_p , 0.25% and 0.5% (0.4% for 10k). Samples with different surfactant concentrations γ have been prepared, where $\gamma = m_{\text{surfactant}} / (m_{\text{water}} + m_{\text{decane}} + m_{\text{surfactant}})$, m_i being the added mass of component i . The membrane volume fraction Ψ is obtained by an analogous expression to γ where the mass of each component is divided by its bulk density. In film contrast, γ and Ψ are almost identical. Phase diagrams have been determined for the different surfactant and homopolymer concentrations. The fish-tail point, where the bicontinuous one-phase region and the three-phase regions meet, shifts towards higher surfactant concentration, when homopolymers are added, i.e., more surfactant is needed to emulsify a certain amount of water and oil. An example to illustrate this shift is presented in Fig. 2 for the case of 5k homopolymers. The film contrast samples used in this study are described in Table I, with the characteristic length scales taken from SANS measurements of the equivalent bulk contrast samples. It has to be pointed out that using deuterated components (D_2O , d -decane) results in a shift of the phase diagram of about 2 °C towards lower temperatures compared to a purely protonated microemulsion,^{6,8} but the surfactant concentration of the fish-tail point is not affected. The viscosities of the different water-PEO and decane-PEP solutions as well as the temperature dependence of the viscosities have been measured with a KPG-Ubbelohde viscosimeter from SCHOTT. The viscosities of pure water¹⁵ and decane¹⁶ have been taken from the literature. To account for the higher

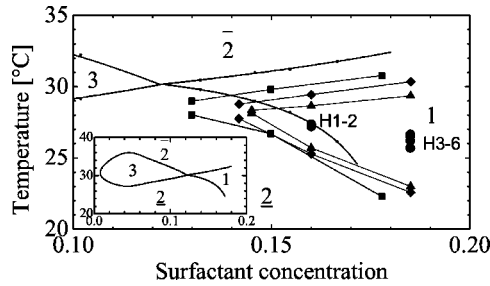


FIG. 2. Phase diagram close to the fish-tail point of a pure microemulsion (H_2O - h -decane- C_{10}E_4) (thin points), a microemulsion in film contrast (D_2O - d -decane- C_{10}E_4 , ■), and microemulsions in film contrast with added homopolymer (PEP₅, PEO₅; 0.25%, ♦ and 0.5%, ▲). The use of deuterated instead of hydrogenated components in film contrast shifts the phase diagram towards lower temperatures. Homopolymers shift the fish-tail point towards higher surfactant concentration, e.g., from about 12.5% surfactant concentration for pure microemulsions to 14.5% at 0.5% homopolymer concentration. The actual positions of the NSE measurements are indicated by ●. The inset shows the complete fishlike phase diagram.

viscosities of the deuterated liquids ($\sim 24\%$ for D_2O , $\sim 6\%$ for d -decane¹⁷), a correction factor of 1.15 has been applied to η_{eff} for the film contrast samples. Since the mode relaxation rate $\omega(k)$ of the free membrane Zimm dynamics is¹⁸

$$\omega(k) = \frac{\kappa k^3}{4\eta_{\text{eff}}} = \frac{\kappa k^3}{2(\eta_{\text{oil}} + \eta_{\text{water}})}. \quad (5)$$

Here, $\eta_{\text{eff}} = (\eta_{\text{oil}} + \eta_{\text{water}})/2$ will be considered, where η_{oil} and η_{water} are the viscosities of the corresponding water-PEO and oil-PEP solutions and k is the undulation wave vector. Here we point out that the momentum transfer \vec{q} , as set in the scattering experiments, is different from the undulation mode vector \vec{k} . As Eq. (8) below illustrates, the scattering $S(q, t)$ contains contributions from a broad range of \vec{k} . The microemulsions have been measured close to the fish-tail point (at a temperature corresponding to the arithmetic average between the lower and upper boundary temperature of the one-phase region). The average viscosities and the corresponding temperatures are noted in Table II. The effect of homopolymers on the phase diagram can be seen in Fig. 2.

The pure microemulsion samples and the samples containing PEP_x-PEO_y diblock copolymers are described elsewhere in detail.^{4,8} Mihailescu *et al.*⁴ studied the dynamics of these samples with NSE and dynamic light scattering. Their parameters important for this study are compiled in Table III. The diblock copolymers are anchored in the membrane,⁶ therefore the effect on the viscosity cannot be determined

TABLE I. Sample compositions of microemulsions with homopolymers.

System	γ	Φ_p	HP type	$\xi(\text{nm})$	$d(\text{nm})$	$\kappa_{\text{SANS}}/k_B T$
H1	0.160	0.0025	5K	12.2	24.9	0.42
H2	0.160	0.0050	5K	11.7	25.0	0.40
H3	0.185	0.0025	5K	10.7	20.6	0.45
H4	0.185	0.0050	5K	10.1	20.6	0.42
H5	0.185	0.0025	10K	8.3	20.6	0.34
H6	0.185	0.0040	10K	7.1	20.5	0.30

TABLE II. Sample parameters.

System	\bar{T} (°C)	$\eta_{\text{eff}} \times 10^{-3}$ [kg/(m s)]	$\eta_{\text{eff}}(\text{film}) \times 10^{-3}$ [kg/(m s)]
H1	27.36	0.86	1.00
H2	27.20	0.90	1.05
H3	26.50	0.88	1.02
H4	26.20	0.92	1.07
H5	26.65	0.89	1.03
H6	25.70	0.94	1.10

from bulk measurements as in the case of homopolymers. The effective viscosity of the surrounding fluid has been taken as the average of pure water and oil.

It will be pointed out in Sec. IV that the correlation length ξ plays an important role in the evaluation of the data and has been reevaluated by careful interpolation of results from SANS measurements on series of microemulsions with varying diblock-copolymer concentration and varying membrane volume fraction, respectively.¹² A special case is sample F3 in Table III, where $d\gamma$ (with d determined by SANS) does not stay at the same value as the other samples, as it should be according to $d \sim \Psi^{-1}$, a reason for this may be that the composition is very close to the phase boundary to the lamellar phase.

B. Neutron scattering

The neutron scattering experiments have been performed at the FRJ2-Research Reactor of the Forschungszentrum Jülich. We performed NSE experiments¹⁹ at the NSE-Spectrometer²⁰ NSE-FRJ2 and the SANS experiments at the SANS-facility KWS2-FRJ2. The samples for the NSE experiments were filled in quartz cuvettes with a thickness of 2 mm. For the SANS experiments, 1 mm cuvettes have been used. In both experiments, the temperature of each sample has been adjusted so that the samples were in the one-phase region of bicontinuous microemulsions exactly in the middle between upper and lower phase boundary temperatures (see Table II). The NSE experiments have been performed at a number of q values ranging from 0.5 nm^{-1} to 2.8 nm^{-1} . Since these bicontinuous microemulsions have a large (coherent) scattering cross section, comparatively large scattering angles are accessible, before the incoherent background

TABLE III. Sample compositions of microemulsions from Ref. 4 with refined ξ : pure ($\delta=0$) and with added diblock copolymers ($\delta>0$) with $\delta = m_{\text{diblock}}/(m_{\text{surfactant}} + m_{\text{diblock}})$.

System	γ	δ	ξ (nm)	d (nm)	$\eta_{\text{eff}}(\text{film}) \times 10^{-3}$ [kg/(m s)]
F1	0.130	0	16.2	32.3	0.94
F2	0.150	0	14.6	26.8	0.94
F3	0.178	0	9.6	16.2	0.97
F4	0.075	0.050	30.4	61.5	0.93
F5	0.100	0.050	23.6	40.5	0.94
F6	0.131	0.050	21.4	32.3	0.94
F7	0.150	0.050	18.9	27.0	0.97

level prevents an efficient data collection. The interpretation in terms of available theoretical models requires that $q \gg q_0$.

III. THEORETICAL DESCRIPTION

The interpretation of experimental data relies on a theoretical expression of the dynamic structure factor $S(q, t)$ for a bicontinuous microemulsion in order to get information on parameters such as the bending constants. Zilman and Granek developed a model describing the interface in terms of finite membrane patches in random orientation,²¹ with the most simple dispersion relation of the undulation modes of a free planar membrane in a viscous liquid,²² $\omega(k) = (\kappa/4\eta)k^3$, where η is the effective solvent viscosity. They found an approximative expression for the dynamic structure factor for bicontinuous microemulsions at large $q (q \gg q_0)$,

$$S(q, t) \approx S(q) \exp(-(\Gamma_q t)^\beta) \quad (6)$$

with $\beta = 2/3$ and the q -dependent relaxation rate Γ_q ,

$$\Gamma_q = 0.025 \gamma_\kappa \left(\frac{k_B T}{\kappa} \right)^{1/2} \frac{k_B T}{\eta} q^3. \quad (7)$$

Here, κ is the bending elasticity modulus, and $\gamma_\kappa \approx 1 - 3(k_B T/4\pi\kappa) \ln(q\xi) \rightarrow 1$ for $\kappa \gg k_B T$.²³ The somewhat counterintuitive dependence of Γ_q on κ in Eq. (7) is due to the fact that not only the undulation relaxation rate [Eq. (5)] is modified, but also the undulation amplitude. A stiffening of the membrane leads to an increase in $\omega(k)$ and a decrease in the amplitude, finally resulting²¹ in $\Gamma_q \propto \kappa^{-1/2}$. The prefactor in Eq. (7), however, depends on additional approximations and fails to yield reasonable values for low κ values as in our case.

A complete numerical evaluation of the model of Zilman and Granek yields a dynamic structure factor as described in Ref. 4,

$$S(q, t) \propto \int_0^1 d\mu \int_0^{r_{\max}} dr r J_0(qr\sqrt{1-\mu^2}) \times \exp \left[-k_B T / (2\pi\kappa) q^2 \mu^2 \right] \times \int_{k_{\min}}^{k_{\max}} dk \frac{1 - J_0(kr) e^{-\omega(k)t}}{k^3}, \quad (8)$$

where the real space upper cutoff is set to $r_{\max} = \pi/k_{\min}$ $= \xi/\epsilon$, $\epsilon \approx 1$ (see below) and the integration variable μ is the cosine of the angle between q and the membrane surface normal. The only free parameter in this equation is the bending modulus in the dispersion relation, which will be denoted κ_{NSE} . The upper cutoff of the mode wave vector, $k_{\max} = \pi/a$ with the membrane thickness $a \approx 1.2$ nm, accounts for the finite size of the surfactant molecules, but has only a marginal influence on the result. By integrating over the undulation mode wave vectors k (not identical to the scattering momentum transfer q , which is fixed by the experimental conditions), all contributions from undulation modes are explicitly taken into account. Therefore, the bare bending modulus is to be used here for κ . The lower cutoff of the mode wave vector, k_{\min} , plays an important role in the evalu-

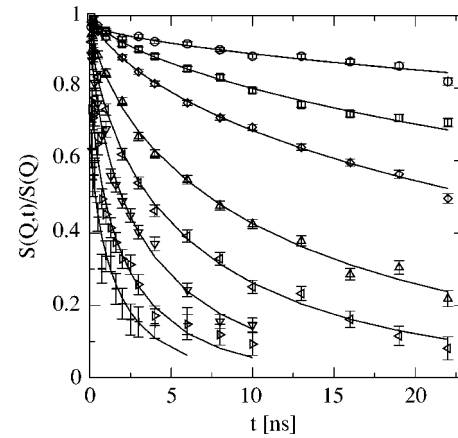


FIG. 3. NSE measurements for $q = 0.5, 0.8, 1.0, 1.4, 1.7, 2.0, 2.4, 2.8$ nm⁻¹ for a sample with 18.5% surfactant and 0.5% PEP₅/PEP₅ and fits to the individual spectra with Eq. (6).

ation of Eq. (8). A detailed discussion has been carried out in Ref. 4. As a natural choice of the cutoff, $k_{\min} = \epsilon\pi/\xi$ with $\epsilon = 1$ has been proposed, and it has been shown that the resulting value of κ_{NSE} is consistent with SANS results, when choosing the scaling parameter $1 \leq \epsilon \leq 1.3$. In this paper, in order to calibrate the method, the value of ϵ has been fixed by fitting Eq. (8) to the experimental data of an arbitrarily chosen sample (H1), such that the condition $\kappa_{\text{NSE}} = \kappa_{\text{bare}}$ is met, i.e., the SANS and NSE results are set equal for this sample, with ϵ being the only free parameter in the “calibration run” of the fitting procedure. For all other samples, the thus determined value of $\epsilon = 1.126$ has been taken, leaving now only κ_{NSE} as the free fit parameter.

IV. RESULTS AND DISCUSSION

A. Direct effects on the relaxation rate Γ_q

Experimental results of a NSE measurement on the sample with a surfactant concentration of 18.5% and 0.5% PEP₅/PEO₅ are presented in Fig. 3. The fits to the experimental data are individually fitted stretched exponential functions [Eq. (6)], with the relaxation rate Γ and the amplitude as the free parameters. The functional form, Eq. (6), of a stretched exponential function with $\beta = 2/3$ and $\Gamma_q \sim q^3$ only holds in the q range of $q \gg q_0$ (see Fig. 4).

In that regime, we consider the reduced relaxation rate $\Gamma^* = (\Gamma_q/q^3)(\eta(T)/k_B T)$, where viscosity effects and the ex-

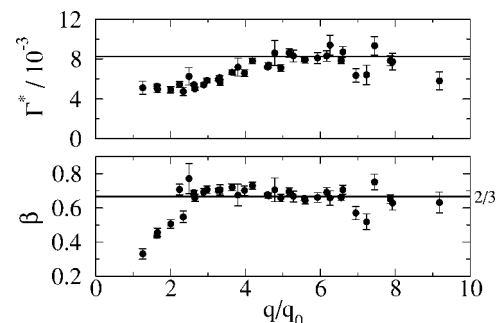


FIG. 4. Parameters Γ^* and β from the fits of Eq. (6) to the data of Fig. 3. Γ^* and $\beta = 2/3$ are shown as straight lines in the graphs.

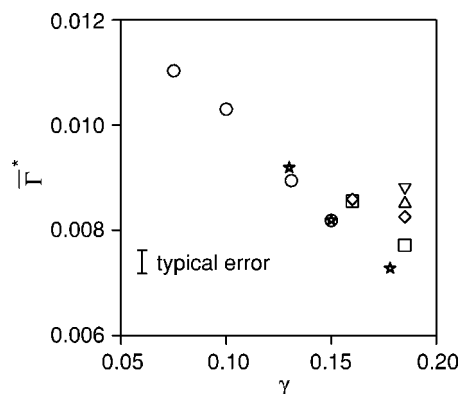


FIG. 5. Average reduced relaxation rate $\bar{\Gamma}^*$ as a function of surfactant concentration (mass fraction γ). While no significant difference has been found between the pure microemulsion (*) and one with diblock copolymers (○), homopolymer addition to the pure microemulsion resulted in an increase in $\bar{\Gamma}^*$. (Homopolymer concentration and type: □ 0.25%, 5 K; ◇ 0.5%, 5 K; △ 0.25%, 10 K; ▽ 0.4%, 10 K).

pected asymptotic q dependence have been eliminated. By taking the average value $\bar{\Gamma}^*$ of $\Gamma^*(q)$ over the range $4q_0 \leq q$ where Γ^* is virtually constant, the statistical accuracy is improved. Figure 4 shows the results for $\bar{\Gamma}^*$ for the sample of Fig. 3. A fit where also the parameter β has been optimized confirms that $\beta=2/3$. It is expected that the dynamics of the surfactant membranes, measured with NSE, is modified by the addition of diblock copolymers or homopolymers, due to changes of κ on the one hand and of the effective viscosity of the surrounding fluids on the other hand. In the case of diblock copolymers, the phase behavior and SANS results show that the bending rigidity is increased as predicted by theory.¹² According to Eq. (7), this should decrease the relaxation rate with respect to the pure microemulsion. However for the tethered diblocks, it is not clear how to quantify their effect on the viscosity and it has been not explicitly accounted for in the previous work.⁴ In a previous series of NSE experiments it has been found that only little influence of block copolymer addition on the raw relaxation rates can be observed,⁴ i.e., effects on the bending modulus and on the viscosity seem to cancel each other to some extent.

The situation is different for homopolymers. SANS experiments showed a decrease of κ_R with increasing homopolymer concentration and increasing homopolymer chain length. The viscosity increases with homopolymer addition, as has been assessed by bulk measurements of the respective oil and water solutions. Hence, when homopolymers are added, it is possible to account for the viscosity change and the full effect of η can be eliminated in $\bar{\Gamma}^*$. According to Eq. (7), the remaining influence of κ on the relaxation rate should lead to an increase of $\bar{\Gamma}^*$. The new results on microemulsions with added homopolymers are compared to those on pure microemulsions and microemulsions where the surfactant membrane has been decorated with diblock copolymers. The influence of these three types of microemulsions on the average reduced relaxation rate $\bar{\Gamma}^* = \langle \Gamma^* \rangle_{q>4q_0}$ is pointed out in Fig. 5. The viscosity has been taken as the average between decane/PEP and water/PEO. A significant increase of $\bar{\Gamma}^*$ on homopolymer addition is indeed

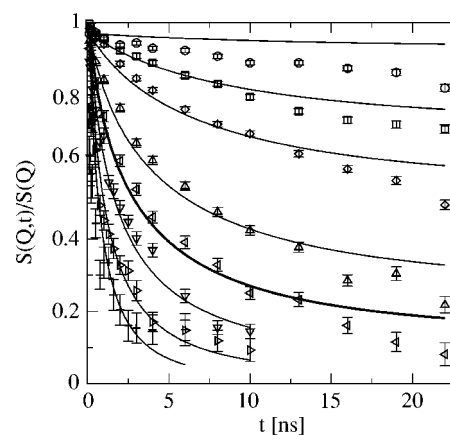


FIG. 6. Comparison of the results from Eq. (8) with the NSE measurements as in Fig. 3 for one parameter set for all curves. It was determined by fitting the curve at $q=1.7 \text{ nm}^{-1}$ (thick solid line) to the experimental data. At high q , the experimental data are described well by the theory, while deviations are observed at low q , where the model assumptions of the Zilman–Granek theory no longer are in reasonable agreement with the bicontinuous structure.

observed, depending on the homopolymer concentration and its molecular weight. The effect gets stronger for higher concentration and higher molecular weight. Note the strong dependence of $\bar{\Gamma}^*$ on γ even when no change of the interface (i.e., κ) by added polymers is anticipated.

B. Derived effects on the bending modulus κ

The values of κ deduced from Eq. (7) are approximately one order of magnitude too high—as already observed in Ref. 4—compared with the values measured by SANS. It was therefore found necessary to evaluate the NSE curves with the full numerically integrated dynamic structure factor [Eq. (8)] in order to obtain more reliable values of κ_{NSE} . The calculated $S(q,t)$ together with the experimental data for one sample are presented in Fig. 6. Also the direct integration [Eq. (8)] still corresponds to the original model of free membrane patches of Zilman–Granek and is expected to be valid only at high q . The fits of κ were therefore performed using data with $q > 4q_0$ only. At lower q , deviations indicate the limits of the model. Figure 7 shows the dependence of κ_{NSE} on the surfactant mass fraction γ for the different types of bicontinuous microemulsions (pure, with diblock copolymers, with homopolymers). The correlation length plays an important role in the evaluation procedure used here via k_{min} . The values of ξ have therefore been reevaluated for the pure microemulsions using the same procedure as for the samples with homopolymers. For the diblock polymers, interpolations with correction terms determined by Endo *et al.*⁶ have been applied to get accurate ξ values (see Table III). In order to compare the obtained values for κ_{NSE} to SANS results, the renormalization correction has been applied to κ_{SANS} . In Fig. 8, the renormalized modulus, $\kappa_R = \kappa_{\text{SANS}}$, and the bare modulus, $\kappa_{\text{SANS}} - 3/(4\pi)\ln(\Phi)$, are presented. A good agreement between the de-renormalized SANS result and κ_{NSE} has been found for pure and homopolymer microemulsions, for the diblock microemulsions a slightly higher value has been obtained with NSE than with SANS. The samples *H5* and *H6*

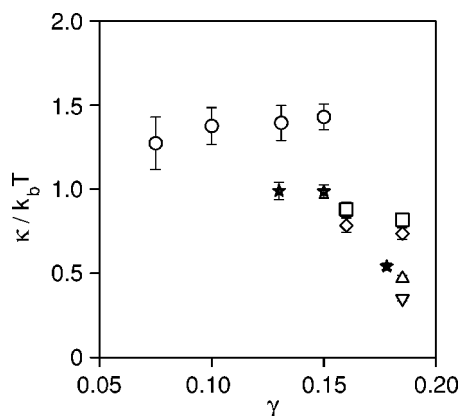


FIG. 7. κ_{NSE} obtained by fitting Eq. (8) to the experimental data (pure microemulsion, \star ; microemulsion with diblock polymers, \circ ; with homopolymers, \square 0.25%, 5 K; \diamond 0.5%, 5 K; \triangle 0.25%, 10 K; ∇ 0.4%, 10 K), as a function of the surfactant concentration γ .

and the pure microemulsion at $\gamma=0.178$ are close to the lamellar phase in the phase diagram. Inhomogeneities in the bicontinuous phase may be induced which may explain the deviating value of κ_{NSE} .

The hypothesis that it is virtually the bare bending modulus of the membrane that is deduced directly from NSE spectra can be further tested by comparing the results obtained above with an evaluation of the NSE data with a κ with length scale dependent renormalization. In the literature^{12,14} also the concept of a length scale dependent renormalization is found, applied to the fluctuation spectrum of membrane undulation this would suggest the mode wavelength $2\pi/k$ as renormalization length. Including such a renormalization term equivalent to that of Eq. (4) in κ used in the dispersion relation, $\omega(k)$ leads to the following relation:

$$\omega(k) = \frac{\kappa k^3}{4\eta_{\text{eff}}} = \left[\kappa_{\text{bare}} - \frac{3}{4\pi} \ln\left(\frac{2\pi}{ak}\right) \right] \frac{k^3}{4\eta_{\text{eff}}}. \quad (9)$$

Instead of the membrane volume fraction $\Psi \sim 1/d$ in Eq. (4), the undulation mode vector k determines the renormalization length scale (with a the size of the surfactant molecule). Using this dispersion relation in the integral equation (8)

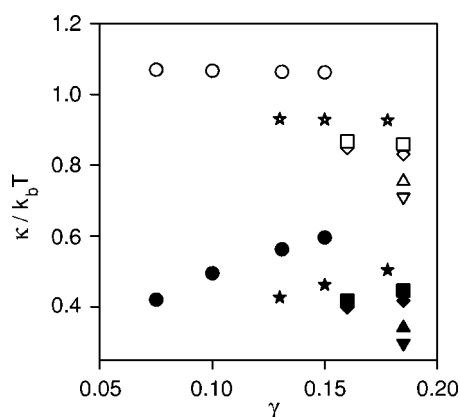


FIG. 8. κ_{SANS} (filled symbols) and after correction for renormalization (open symbols) (pure microemulsion, \star ; microemulsion with diblock polymers, \circ ; with homopolymers, \square 0.25%, 5 K; \diamond 0.5%, 5 K; \triangle 0.25%, 10 K; ∇ 0.4%, 10 K), as a function of the surfactant concentration γ .

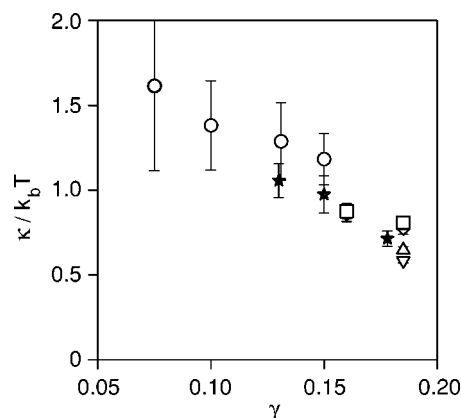


FIG. 9. κ_{NSE} obtained by fitting Eq. (8) to the experimental data, including renormalization in the dispersion relation (pure microemulsion, \star ; microemulsion with diblock polymers, \circ ; with homopolymers, \square 0.25%, 5 K; \diamond 0.5%, 5 K; \triangle 0.25%, 10 K; ∇ 0.4%, 10 K), as a function of the surfactant concentration γ . The renormalization effect is overestimated in this case, leading to a γ dependence of κ .

leads to a bare κ where possible renormalization effects on long wavelength undulations have been corrected. The resulting values from fits to the NSE data of the bending modulus are shifted by $\sim +0.5k_B T$ with respect to those determined without renormalization correction. Furthermore, an increase in surfactant concentration leads to a decrease of κ , whereas the dispersion relation, Eq. (5), leads to a constant κ , as would be expected for the bare bending modulus of the membrane. The overall shift of the values can be compensated by a change of the frequency cutoff parameter ϵ from 1.126 to 2. The result of the evaluation with Eq. (9) and with $\epsilon=2$ is shown in Fig. 9. The decreasing bending rigidity with surfactant concentration indicates that in the case of NSE the renormalization effect is overestimated by the applied renormalization correction, whereas the dispersion relation, Eq. (5), leads to the expected constant value for κ .

We conclude therefore that NSE measures mainly the bare bending modulus of the membrane (the bare bending modulus κ_0 plus effects of diblock copolymers and homopolymers), i.e., the NSE fluctuation spectra take into account all undulations up to an upper cutoff equivalent to the membrane thickness, the relevant modulus here is κ_{bare} . In contrast the SANS analysis relies on the average structure at large scale d or ξ , therefore, the resulting κ value is the renormalized one. The difference in the concentration dependence, i.e., scale dependence, and values of bending moduli measured by SANS, κ_{SANS} , and that measured by NSE, κ_{NSE} , therefore is the manifestation of the different length scale of the renormalization.¹²

V. CONCLUSION

The bare bending moduli as obtained from NSE measurements of the relaxation dynamics of membrane fluctuations in bicontinuous microemulsions depend on the addition of polymers. Addition of two homopolymers that are macromolecular analogs of the both sides of the surfactant to the water and oil phase, respectively, reduce the bending modulus. The reduction increases with concentration from 0.25% to 0.5% and molecular weight. Thereby the bare modulus of

the pure surfactant layer is reduced from about $1k_B T$ to $0.5k_B T$. The data on the addition of diblock copolymers that are direct polymeric analogs of the whole surfactant molecules from Ref. 4 were included into the κ evaluation and led to κ values that are about $0.3k_B T$ higher than those of the pure surfactant system. As one would expect the series of constant diblock fraction (5%) in the surfactant phase and different total surfactant concentration, i.e., varying structure length, yields virtually equal κ values for the different concentrations. Since the nature of the surfactant interface should be the same within this series, this is the expected result. Here it is noteworthy to point out that the raw data, i.e., the reduced relaxation rates, vary significantly and more than by mere polymer addition within this series. Only the inclusion of the correlation length, which directly depends on the concentration, into the evaluation using the full integration in terms of cutoffs of mode spectra and the related lateral extension is able to describe this effect on Γ^* properly. The simplified approximations, Eqs. (6) and (7)—in particular if $\gamma_\kappa=1$ is assumed—must fail since no dependence on the correlation length ξ is left. To facilitate the application of the full evaluation scheme in future applications, an easy to use procedure without the need to fit with the nested integral is given in the Appendix.

The results for κ that are obtained from the SANS data, as presented in Ref. 8 on the first hand show a different behavior. This is readily understood as consequence of the different renormalization states of κ_{SANS} and κ_{NSE} . The SANS features on the structural length scale used to extract κ depend on the renormalized value whereas the fluctuation dynamics is modeled using undulation modes of all possible lengths. The latter lead to the bare bending moduli from the NSE evaluation. Indeed this leads the subtraction of the expected renormalization effect, Eq. (4), from κ_{SANS} to the same qualitative dependence of the bending moduli on polymer addition as found from the NSE result.

The assumption that NSE experiments directly measure the bare κ is tested by including a wavelength dependent renormalization term also in the integral form of the NSE evaluation. The resulting κ_{NSE} values vary with the surfactant concentration, in contrast to what would be expected for the bare bending modulus κ_0 . This indicates that κ_0 has to be taken into account directly in the integral form of the Zilman–Granek.

The absolute magnitude of the polymer effect obtained from the NSE results is somewhat larger than that seen in the de-renormalized SANS results. This indicates that still the methodology to extract κ from either $S(q)$ from SANS or $S(q,t)/S(q)$ is yet not perfect. Here both, the limited realism of the membrane patch ensemble model of Zilman and Granek and the further and ignored influences contained in the function $\Theta(\kappa_{\text{SANS}}, \Psi)$ occurring in the interpretation of SANS data may play a role. Improvements of the accuracy and reliability of these values will be the matter of further investigations.

The qualitative response of the observed bending moduli on homopolymer and diblock-copolymer addition is in accordance with theoretical predictions.^{9,24} Where the effect of diblock addition is of the same magnitude as predicted,^{4,24}

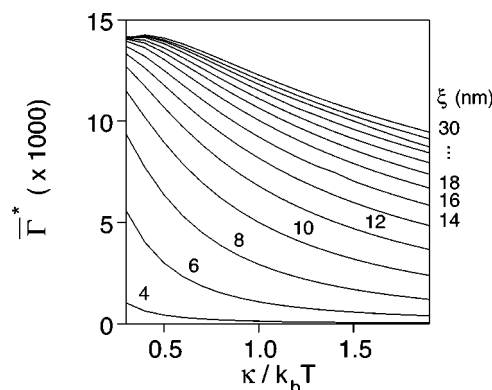


FIG. 10. The parameter Γ^* plotted as a function of κ and ξ .

the homopolymer effect is much larger than it would be inferred from the available theory.⁹ The latter effect has already been discussed in Ref. 8, taking the NSE results it would be even larger.

ACKNOWLEDGMENT

The authors would like to thank G. Gompper for fruitful discussions.

APPENDIX: SIMPLIFIED DETERMINATION OF κ

The evaluation of the integral in Eq. (8) in order to obtain κ is a rather complicated procedure. Here we present a method which allows us to obtain reliable values of κ from a data evaluation with a stretched exponential function. $S(q,t)$ has been calculated using Eq. (8) for a set of κ and ξ values. It then has been fitted with a stretched exponential function to obtain Γ_q . Finally, $\Gamma^* = (\Gamma_q/q^3)[\eta(T)/k_B T]$ has been deduced which eliminates the q and η dependence from the relaxation rate (Fig. 10). If ξ is known, e.g., from SANS measurements and Γ^* is deduced from NSE data, it is possible to infer the corresponding κ_{NSE} from this plot. This procedure leads to κ values which are within $\pm 20\%$ of the fit results obtained using Eq. (8) directly for data for $q > 4q_0$.

¹M. Kahlweit, R. Strey, R. Schomaecker, and D. Haase, *Langmuir* **5**, 305 (1989).

²G. Gompper and G. Schick, in *Phase Transitions and Critical Phenomena*, edited by C. Domb and J. Lebowitz (Academic, London, 1994), Vol. 16.

³W. Helfrich, *Z. Naturforsch. C* **28**, 693 (1973).

⁴M. Mihailescu, M. Monkenbusch, H. Endo *et al.*, *J. Chem. Phys.* **115**, 9563 (2001).

⁵H. Endo, J. Allgaier, G. Gompper, B. Jakobs, M. Monkenbusch, D. Richter, T. Sottmann, and R. Strey, *Phys. Rev. Lett.* **85**, 102 (2000).

⁶H. Endo, M. Mihailescu, M. Monkenbusch *et al.*, *J. Chem. Phys.* **115**, 580 (2001).

⁷B. Jakobs, T. Sottmann, R. Strey, J. Allgaier, L. Willner, and D. Richter, *Langmuir* **15**, 6707 (1999).

⁸D. Byelov, H. Frielinghaus, O. Holderer, M. Monkenbusch, J. Allgaier, and D. Richter, *Langmuir* **20**, 10433 (2004).

⁹A. Hanke, E. Eisenriegler, and S. Dietrich, *Phys. Rev. E* **59**, 6853 (1999).

¹⁰M. Teubner and R. Strey, *J. Chem. Phys.* **87**, 3195 (1987).

¹¹S.-H. Chen, S.-L. Chang, and R. Strey, *J. Chem. Phys.* **3**, 1907 (1990).

¹²G. Gompper, H. Endo, M. Mihailescu *et al.*, *Europhys. Lett.* **56**, 683 (2001).

¹³L. Golubović, *Phys. Rev. E* **50**, R2419 (1994).

¹⁴L. Peliti and S. Leibler, *Phys. Rev. Lett.* **54**, 1690 (1985).

¹⁵*Handbook of Chemistry and Physics*, 57th ed. (CRC, Cleveland, 1976).

- ¹⁶R. Berg and M. Moldover, J. Chem. Phys. **6**, 3687 (1987).
- ¹⁷L. Andrussov and K. Schäfer, in *Eigenschaften der Materie in ihren Aggregatzuständen*, edited by K. Schäfer (Springer, Berlin, 1969), Vol. 5A, pp. 128–157.
- ¹⁸T. Schilling, O. Theissen, and G. Gompper, Eur. Phys. J. E **4**, 103 (2001).
- ¹⁹F. Mezei, *Neutron Spin Echo*, edited by F. Mezei (Springer, Berlin, 1980).
- ²⁰M. Monkenbusch, R. Schaetzler, and D. Richter, Nucl. Instrum. Methods Phys. Res. A **399**, 301 (1997).
- ²¹A. Zilman and R. Granek, Phys. Rev. Lett. **77**, 4788 (1996).
- ²²R. Messenger, P. Basser, and G. Porte, J. Phys. (France) **51**, 1329 (1990).
- ²³F. Brochard and J. Lennon, J. Phys. (Paris) **11**, 1035 (1975).
- ²⁴C. Hiergeist and R. Lipowsky, J. Phys. II **6**, 1465 (1996).